



Third DWF1 paralog in Solanaceae, sterol Δ^{24} -isomerase, branches withanolide biosynthesis from the general phytosterol pathway

Eva Knoch^a, Satoko Sugawara^a, Tetsuya Mori^a, Christian Poulsen^b, Atsushi Fukushima^a, Jesper Harholt^b, Yoshinori Fujimoto^c, Naoyuki Umemoto^a, and Kazuki Saito^{a,d,1}

^aRIKEN Center for Sustainable Resource Science, Yokohama, Kanagawa 230-0045, Japan; ^bCarlsberg Research Laboratory, 1778 Copenhagen, Denmark; ^cDepartment of Chemistry, Tokyo Institute of Technology, Meguro, Tokyo 152-8550, Japan; and ^dGraduate School of Pharmaceutical Sciences, Chiba University, Chuo-ku, Chiba 260-8675, Japan

Edited by Harry J. Klee, University of Florida, Gainesville, FL, and approved July 9, 2018 (received for review May 2, 2018)

A large part of chemodiversity of plant triterpenes is due to the modification of their side chains. Reduction or isomerization of double bonds in the side chains is often an important step for the diversification of triterpenes, although the enzymes involved are not fully understood. Withanolides are a large group of structurally diverse C₂₈ steroidal lactones derived from 24-methylenecholesterol. These compounds are found in the Indian medicinal plant *Withania somnifera*, also known as ashwagandha, and other members of the Solanaceae. The pathway for withanolide biosynthesis is unknown, preventing sustainable production via white biotechnology and downstream pharmaceutical usages. In the present study, based on genome and transcriptome data we have identified a key enzyme in the biosynthesis of withanolides: a DWF1 paralog encoding a sterol Δ^{24} -isomerase (24ISO). 24ISO originated from DWF1 after two subsequent duplication events in Solanoideae plants. Withanolides and 24ISO appear only in the medicinal plants in the Solanoideae, not in crop plants such as potato and tomato, indicating negative selection during domestication. 24ISO is a unique isomerase enzyme evolved from a reductase and as such has maintained the FAD-binding oxidoreductase structure and requirement for NADPH. Using phylogenetic, metabolomic, and gene expression analysis in combination with heterologous expression and virus-induced gene silencing, we showed that 24ISO catalyzes the conversion of 24-methylenecholesterol to 24-methylidestmosterol. We propose that this catalytic step is the committing step in withanolide biosynthesis, opening up elucidation of the whole pathway and future larger-scale sustainable production of withanolides and related compounds with pharmacological properties.

sterol biosynthesis | *Withania somnifera* | sterol 24-isomerase | withanolides | pathway evolution

Plants produce a huge array of structurally diversified, specialized metabolites that are involved in the interaction between plants and their environment. Triterpenoids/steroids are one of the most numerous and diverse groups of plant metabolites (1). Often their structural diversity lies in the modification of side chains, which are modified by formation, reduction, and isomerization of double bonds. Withanolides are a group of secondary metabolites, found mostly in plants from the Solanaceae family, that contains more than 600 structurally distinct compounds (2). The best-known plant to produce withanolides is *Withania somnifera*, also known as Indian Ayurvedic ashwagandha, a medicinal plant used for over 3,000 y and also relevant for modern medicine (3). A number of withanolides show promising pharmacological properties for the treatment of inflammation-mediated chronic diseases including cancer, arthritis, and autoimmune and neurodegenerative diseases (4). The diversity of structures and activities within this group of compounds makes it a promising source for novel compounds with potential pharmaceutical and nutraceutical uses.

The general structure of withanolides (CAS name: 22-hydroxyergostan-26-oic acid 26,22-lactone) is C₂₈ ergostane with

a side chain that forms a δ -lactone ring between C22 and C26 (5). Based on their steroidal backbone, withanolides share an upstream biosynthetic pathway with general phytosterols; 24-methylenecholesterol (6) and 24-methylidestmosterol (7) are precursors of withanolides, but not 24-(R/S)-24-methylcholesterol (campesterol and dihydrobrassicasterol) (6). The 24-methylenecholesterol is also an intermediate in the biosynthesis of brassinolides, where DWF1 catalyzes the conversion of 24-methylenecholesterol to campesterol, through isomerization of the $\Delta^{24(28)}$ -double bond to $\Delta^{24(25)}$ -double bond yielding the intermediate 24-methylidestmosterol, followed by reduction (8–10) (Fig. 1). The isomerization of 24-methylenecholesterol to 24-methylidestmosterol has been proposed to be a pivotal step in the biosynthesis of withanolides (7), but to date no gene or enzyme has been characterized for this branching step from the general phytosterol pathway.

Potato and tomato, belonging to the Solanaceae family, have two DWF1 homologs named sterol side chain reductase (SSR) 1 and SSR2 (11). SSR1 activity corresponds to DWF1 and reduces 24-methylenecholesterol to campesterol, while SSR2 reduces the C24 double bond of $\Delta^{24(25)}$ -sterols, such as from cycloartenol to

Significance

Withanolides form a major class of plant steroids with unique side-chain modifications. Withanolides are one of the main active components in an Indian Ayurvedic medicinal plant, ashwagandha, which has been used for over 3,000 y. Because of their highly diversified structures, withanolides are promising pharmacological compounds with proven antiinflammatory and anticancer properties. We identified a sterol Δ^{24} -isomerase (24ISO) catalyzing the first committed step in the biosynthesis of withanolides and related compounds. Identification of 24ISO paves the way for targeted manipulations to increase withanolide yields and as a starting point to elucidate the downstream pathway of yet-unknown withanolide biosynthesis. This study also demonstrates how the evolution of enzymes catalyzing double-bond modifications of triterpene side chains lead to diversity in structures and functions.

Author contributions: E.K., N.U., and K.S. designed research; E.K. and S.S. performed research; T.M., C.P., A.F., and Y.F. contributed new reagents/analytic tools; E.K., S.S., T.M., C.P., A.F., and N.U. analyzed data; and E.K., J.H., N.U., and K.S. wrote the paper.

The authors declare no conflict of interest.

This article is a PNAS Direct Submission.

This open access article is distributed under [Creative Commons Attribution-NonCommercial-NoDerivatives License 4.0 \(CC BY-NC-ND\)](https://creativecommons.org/licenses/by-nc-nd/4.0/).

Data deposition: The sequences reported in this paper have been deposited in the GenBank database (accession nos. [MH184042–MH184049](https://accession.ncbi.nlm.nih.gov/1807482115/)).

¹To whom correspondence should be addressed. Email: kazuki.saito@riken.jp.

This article contains supporting information online at www.pnas.org/lookup/suppl/doi:10.1073/pnas.1807482115/-DCSupplemental.

Published online August 6, 2018.

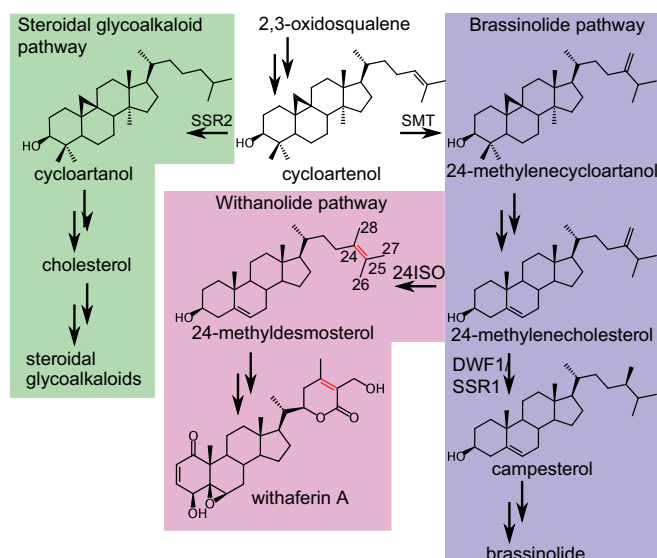


Fig. 1. Overview of the reactions catalyzed by DWF1/SSR1, SSR2, and 24ISO and the proposed role of 24ISO in the biosynthesis of withanolides. Withaferin A is shown as an example of withanolides, and the $\Delta^{24(25)}$ is shown in red. SMT, sterol methyltransferase.

cycloartanol, in the biosynthesis of cholesterol (Fig. 1), the same reaction as catalyzed by the human 24-dehydrocholesterol reductase (DHCR24) (12). This duplication and divergence has also been reported for several other enzymes involved in phytosterol and cholesterol biosynthesis as well (13), demonstrating how new multistep metabolic pathways involved in secondary metabolite biosynthesis may develop from primary metabolic pathways. In this context, it is relevant to address whether a third class of enzyme, besides SSR1 and SSR2, is involved in the isomerization of side-chain double bonds leading to the biosynthesis of withanolides and related compounds.

We have recently analyzed the transcriptomes of two withanolide-producing *Physalis* species, *Physalis alkekengi* and *Physalis peruviana* (14). *P. peruviana* produces withanolide E and related withanolides, while *P. alkekengi* produces physalin B and related physalin-type withanolides. Our analysis of both *Physalis* transcriptomes revealed the presence of three DWF1 homologs in this genus. We hypothesized that the third DWF1 homolog is involved in withanolide biosynthesis. Here we show that the third homolog is a sterol Δ^{24} -isomerase (EC 5.3.3) that catalyzes the conversion of 24-methylenecholesterol to 24-methylidestmasterol in the initial step in the withanolide biosynthesis branching off the general phytosterol pathway (Fig. 1).

Results

Phylogenetic Analysis Indicates the Presence of a Third DWF1 Homolog in Withanolide-Producing Plants. Using the potato StSSR1 and StSSR2 amino acid sequences as queries in a BLAST analysis against 20,689 and 25,751 unigenes in *P. alkekengi* and *P. peruviana*, respectively (14), we identified three matching sequences in each species: PaSSR1, PpSSR1, PaSSR2, PpSSR2, and the homologous sequences designated Pa24ISO and Pp24ISO, which stands for sterol Δ^{24} -isomerase. Likewise, BLAST analysis of *W. somnifera* transcriptome data reassembled from SRA sequences (15, 16) identified three sequences (WsSSR1, WsSSR2, and Ws24ISO). These three proteins contain common domains such as an N-terminal membrane anchor, FMN binding domain (domain architecture ID 11416043), and the Rossmann fold structure and have equal molecular weight of around 65 kDa. Ws24ISO is 79% identical to WsSSR1 and 85% identical to WsSSR2 (*SI Appendix*,

Fig. S1 shows an alignment of Ws24ISO, WsSSR1, and WsSSR2). Based on these findings, we performed phylogenetic analysis of DWF1 homologs from several plants of the Solanaceae family. The result revealed three distinct clades in the SSR family: SSR1, SSR2, and 24ISO/SSR-like (Fig. 2A). SSR1 and SSR2 are present in all analyzed species of the Solanaceae, while 24ISO/SSR-like is a paralog and restricted to a smaller subset. Based on the phylogeny, 24ISO/SSR-like is a sister clade to SSR2, with which they share a higher common ancestor than the common ancestor of SSR1 and SSR2. With the exception of *Petunia*, 24ISO/SSR-like was only detected within the Solanoideae subfamily. Fig. 2B shows the occurrence of withanolides or related compounds reported in the literature and of the 24ISO/SSR-like gene in tribes of the Solanaceae family, indicating a correlation between the presence of 24ISO/SSR-like and withanolides or petuniasterones (C_{28} isoprenoids found in *Petunia*). Withanolides or closely related compounds have been detected in several genera of the Solanoideae subfamily, namely in *Acnistus*, *Brachistus*, *Deprea*, *Discopodium*, *Dunalia*, *Eriolarynx*, *Iochroma*, *Leucophysalis*, *Physalis*, *Salpichroa*, *Tubocapsicum*, *Vassobia*, *Withania*, and *Witheringia* from the Physalineae tribe; *Datura* from the Datureae tribe; *Hyoscyamus* from the Hyoscyameae tribe; *Lycium* from the Lycieae tribe; *Jaborosa* from the Jaboroseae tribe; and *Solanum* from the Solaneae tribe, as well as the genera *Exodeconus*, *Nicandra*, and *Mandragora*, whose positions are unresolved (17, 18).

We identified 24ISO/SSR-like in two members of the Solaneae only, *Solanum melongena* and *Solanum xanthocarpum*; the gene was not found in the genomes of either *Solanum tuberosum* or *Solanum lycopersicum* or available transcriptomes of other *Solanum* species (Fig. 2A). *Sm24ISO/SSR-like* appears to be a pseudogene because it contains a premature stop codon, leaving *Sx24ISO* as the only putative 24ISO/SSR-like in Solaneae. Withanolides have been reported for *Solanum ciliatum* (19) and *Solanum sisymbriifolium* (20) as the only species in this tribe. We could not identify 24ISO/SSR-like in *S. sisymbriifolium* transcriptome available at the 1KP database (21) (no transcriptome or genome information was available for *S. ciliatum*). In *Capsicum annuum*, we identified 24ISO expression exclusively in roots, but no withanolides or related compounds have been reported for any genus within the Capsiceae tribe to date. Surprisingly, we also identified 24ISO in *Petunia*, a plant outside the Solanoideae subfamily, and not known to produce withanolides, but known to accumulate C_{28} isoprenoids known as petuniasterones (22). Another outlier was *Browalia viscosa* in the Cestoideae tribe, which produces withaferin A and nicandrenone (23). It is unknown whether 24ISO is also found in the Cestroideae, as there is no available genomic information.

The 24ISO Is Localized in a Gene Cluster with Other Potential Pathway Genes in *C. annuum*, *Petunia inflata*, and *S. melongena*. SSR1 and SSR2 are both located on chromosome 2 in potato and tomato, more than 10 Mbp apart (11). Of plants that contain 24ISO/SSR-like, only the genomes of *C. annuum* and *S. melongena* have been annotated at the time of this writing (24, 25). The location of *CaSSR1* (Capana02g000339) and *CaSSR2* (Capana02g001326) to chromosome 2 is conserved in *C. annuum*, but *Ca24ISO* (Capana06g002437) is located on chromosome 6. In *S. melongena*, *SmSSR1* (SMEL_002g157630) is located on chromosome 2, *SmSSR2* (SMEL_3Chr00.13147) is not annotated yet, and *Sm24ISO/SSR-like* (SMEL_008g315450) is located on chromosome 8.

In *C. annuum* and *S. melongena*, 24ISO/SSR-like is localized in potential gene clusters with genes encoding cytochrome P450s and 2-oxoglutarate-dependent dioxygenases (2OGDs) (Fig. 3) that might be involved in further metabolism of 24-methylidestmasterol. Among the cytochrome P450s are several that belong to the CYP88 subfamily, which contains known enzymes that hydroxylate triterpenes and diterpenes (26, 27). Likewise, a 2OGD contributes to the biosynthesis of steroidal glycoalkaloids in potato and tomato (28, 29), thus 2OGDs might also be involved in withanolide

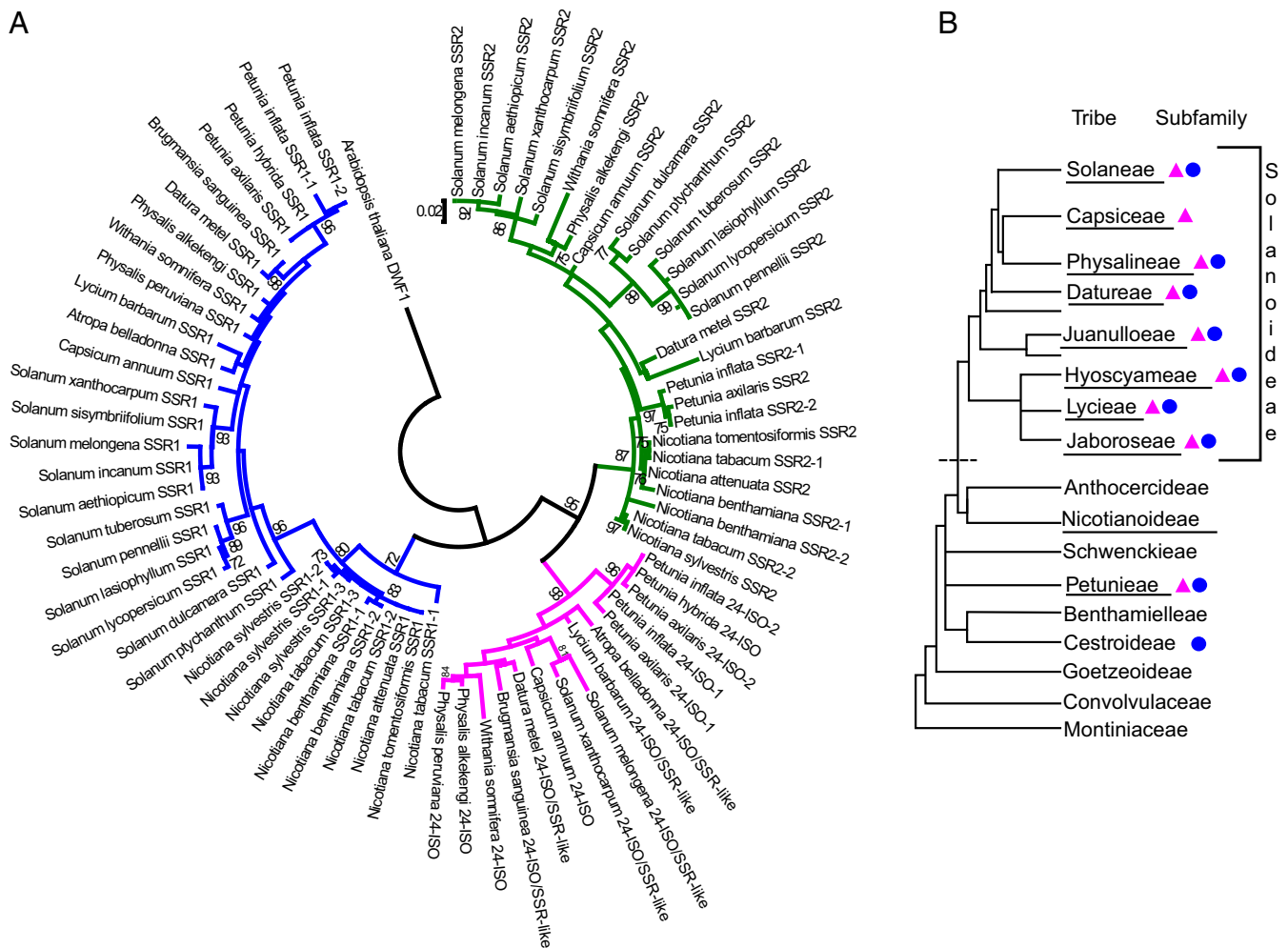


Fig. 2. The 24ISO forms a monophyletic group and occurs in tribes producing withanolides. (A) Phylogenetic analysis of Solanaceae DWF1 homologs. Phylogenetic relationship was inferred using the maximum likelihood method in Mega7. Numbers shown are bootstrap values in percentages (based on 1,000 replicates). *Arabidopsis thaliana* DWF1 was used to root the tree. Solanaceae DWF1 homologs cluster into three distinct clades, SSR1 (blue), SSR2 (green), and 24ISO/SSR-like (magenta). (B) Overview of the occurrence of 24ISO/SSR-like (magenta triangle) and withanolides, or petuniasterones in the case of *Petunia*, (blue dot) in tribes of the Solanaceae. Tribes containing species for which genome or transcriptome data are available are underlined (Fig. 2B data from ref. 63).

biosynthesis. In *S. melongena*, like 24ISO/SSR-like, the cytochrome P450 genes are truncated pseudogenes. In the available genome data for *P. inflata* (30), we identified two copies of 24ISO in a heavily duplicated region containing several cytochrome P450 genes as well as a 2OGD (Fig. 3).

The Expression of 24ISO Correlates with Occurrence of 24-Methyl-desmosterol in Plant Tissues. The $\Delta^{24(25)}$ -double bond (Fig. 1) is a key structural feature commonly found in withanolides. We hypothesized that the 24ISO, which we identified in plants producing withanolides, catalyzes formation of the $\Delta^{24(25)}$ -double bond in withanolide biosynthesis. Because of its homology to SSR1, we proposed that 24ISO catalyzes only the first step of the two-step reaction catalyzed by SSR1, the conversion of 24-methylenecholesterol to the withanolide precursor 24-methyl-desmosterol. We therefore measured 24ISO gene expression levels by qPCR and the amount of 24-methyl-desmosterol in different tissues of several plants containing 24ISO by GC-MS (Fig. 4). Accumulation of 24-methyl-desmosterol largely correlated with the gene expression pattern of 24ISO among species and tissues. The expression of SSR1 and SSR2 differed from the accumulation pattern of 24-methyl-desmosterol (SI Appendix, Fig. S2). Regarding SSR1 and SSR2, among sterols analyzed the level of cholesterol was correlated

with the expression of SSR2, as expected. We did not detect *Sm24ISO* gene expression in any of the tissues analyzed, further indicating that it is indeed a pseudogene.

The 24ISO Expressed in Yeast Converts 24-Methylenecholesterol to 24-Methyl-desmosterol. To directly determine if the 24ISO proteins catalyze conversion of 24-methylenecholesterol to 24-methyl-desmosterol, we expressed Pa-, Ws-, Ph-, and Ca24ISO in the 24-methylenecholesterol-producing T21 yeast strain (11) and analyzed the sterols of transformed yeast strains by GC-MS. Expression of all four 24ISOs individually in the T21 yeast strain correlated with detection of 24-methyl-desmosterol, identified based on comparison of retention time and MS spectra of the 24ISO product to an authentic standard (Fig. 5A and B). Additionally, the four 24ISOs showed weak $\Delta^{24(25)}$ -reductase activity to produce cholesterol in yeast (SI Appendix, Fig. S3). As previously reported for *S. tuberosum* (St) and *S. lycopersicum* (Sl) SSR1 and SSR2 (11), transgenic expression of PaSSR1 and PaSSR2 conferred the ability to produce campesterol and cholesterol, respectively (SI Appendix, Fig. S3).

SSR1 and SSR2 have been described to require NADPH as reductant for their reactions (11). Since 24ISO catalyzed an isomerization reaction with no net redox change, we examined whether NADPH is also required for 24ISO activity. For this purpose, we

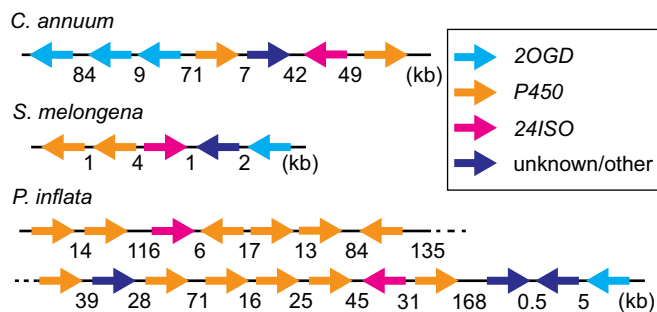


Fig. 3. Possible gene clusters in the genomes of three Solanaceous species. The *24ISO* is localized in potential gene clusters in *C. annuum*, *S. melongena*, and *P. inflata*, containing genes encoding cytochrome P450s and 2OGDs. Genome region from chromosome 6 for *C. annuum*, chromosome 8 for *S. melongena*, and *P. inflata* scaffold 00464 are shown (not to scale), and genes are represented by arrows indicating their orientation in the genome. Numbers below the lines show the distances between genes in kilobases. The two cytochrome P450 genes in *S. melongena* are only short pseudogenes.

expressed *24ISO* in the *erg4* yeast strain. Upon incubation of cell-free homogenates of *24ISO* expressing *erg4* yeast with 24-methylenecholesterol, 24-methylidesmosterol was detected only when NADPH, but not NADP⁺, was present in the reaction mixture (Fig. 5C). No net NADPH consumption was observed compared with empty vector control, indicating that no net reduction takes place. Remaining NADPH in the assay mix after incubation was 46.55% ± 6.36 (*n* = 3) for empty vector and 46.07% ± 1.46 (*n* = 3) for *24ISO* of the original amount.

The *24ISO* Is Indispensable for Withanolide Biosynthesis Through Production of 24-Methylidesmosterol. To further elucidate the activity of *24ISO*, *in planta* experiments were conducted by gain-of-function and loss-of-function strategies. *Nicotiana benthamiana* has no endogenous *24ISO*, and no 24-methylidesmosterol was detected in GC-MS analysis of sterols extracted from wild-type and empty vector control leaves. Transient overexpression of *24ISO* in leaves of *N. benthamiana* led to accumulation of small amounts of 24-methylidesmosterol detected by GC-MS (Fig. 6A). Notably, the precursor 24-methylenecholesterol was reduced to below detection limit in the *24ISO*-expressing leaves (Fig. 6A). Confocal microscopy imaging showed that transiently expressed *24ISO* localized to the ER (Fig. 6B and *SI Appendix*, Fig. S4), corresponding to the reported site for sterol biosynthesis and localization of *SSR1* (31) and *SSR2* (13).

To verify the role of *24ISO* in withanolide biosynthesis, we silenced *24ISO* in young *W. somnifera* plants by virus-induced gene silencing (VIGS). To silence only *24ISO* but not *SSR1* gene expression (*SSR1* sequence is 80% identical to *24ISO*), we designed a construct assembled from three distinct *24ISO* fragments exhibiting high sequence specificity (Fig. 6C and *SI Appendix*, Fig. S5). Off-target silencing of *SSR2* was no concern, as this gene was not expressed in aerial tissues (*SI Appendix*, Fig. S2), and we further confirmed that *SSR2* was not expressed in VIGS control and *24ISO*-silenced plants. Silencing of *24ISO* reduced the content of 24-methylidesmosterol and reciprocally increased the level of 24-methylenecholesterol (Fig. 6D and *SI Appendix*, Fig. S6). Furthermore, liquid chromatography quadrupole TOF MS (LC-QTOF-MS) analysis of withaferin A, the major withanolide in leaves of *W. somnifera* (32), showed that it was significantly reduced in *24ISO*-silenced plants (Fig. 6E and *SI Appendix*, Figs. S6 and S7). The levels of withaferin A in the silenced lines were positively correlated with the expression of *24ISO* (correlation coefficient 0.79). These results

suggest that expression of *24ISO* is necessary for production of 24-methylidesmosterol and withanolide biosynthesis.

Discussion

Although withanolides have been studied for several decades because of their general interest as major pharmacological components of traditional Indian Ayurvedic medicine and because they include promising compounds for modern medicine, their biosynthetic pathway is largely unknown (33). Several studies have reported the effect of manipulation of the general phytosterol pathway on withanolides, but no withanolide-specific activities have, to our knowledge, been identified. One *W. somnifera* glucosyltransferase has been implied to glycosylate both withanolides and phytosterols (34). We have shown here that *24ISO* is a key enzyme in the production of withanolides, catalyzing the committing isomerization of 24-methylenecholesterol to 24-methylidesmosterol. Since withanolides generally contain the $\Delta^{24(25)}$ -double bond in their lactone structures, *24ISO* could be regarded as the committing enzyme for the biosynthetic pathway of this diverse class of plant natural products.

The *24ISO* from four different plant species tested in this study showed comparable activity. Out for the four species, only *W. somnifera* and *P. alkekengi* produce withanolides (17), so the role of *24ISO* in *Petunia hybrida* and *C. annuum* remains speculative. Epoxy $\Delta^{24(25)}$ sterol is a proposed precursor of petuniosterones and has been used in the synthesis of petuniosterones (35). Thus, *24ISO* may be involved in the production of petuniosterones in *P. hybrida*. No withanolides have been reported for *C. annuum*. However, as expression of *Ca24ISO* is exclusive to root tissue, it is possible that as-yet-undiscovered 24-methylidesmosterol-derived metabolites may be present in this tissue.

The *24ISO* is a paralog of *DWF1/SSR1* and *SSR2*. Three proteins encoded by these genes have very similar sequences, including an FMN-binding domain. No crystallographic structures, unfortunately, have been reported on these or similar proteins until now. Therefore, it is difficult to find any features that divide *24ISO* from the reductases for the moment. However, this is an interesting question to address in future investigations. *DWF1* homologs are common throughout the plant kingdom and are

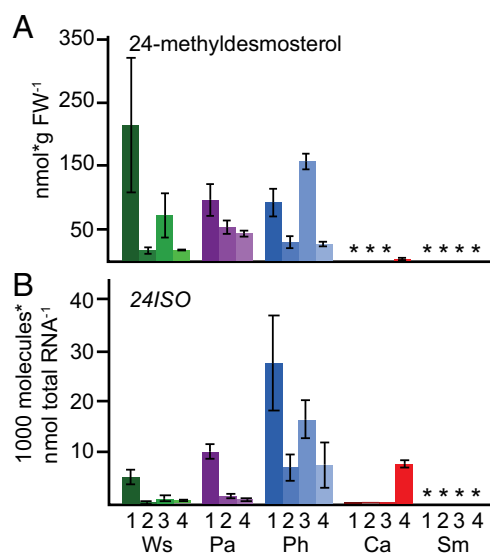


Fig. 4. Correlation of level of 24-methylidesmosterol and expression of *24ISO*. (A) Amount of 24-methylidesmosterol and (B) expression of *24ISO* in *W. somnifera* (Ws), *P. alkekengi* (Pa), *P. hybrida* (Ph), *C. annuum* (Ca), and *S. melongena* (Sm) in young leaves (1), mature leaves (2), flowers (3) and root (4). *Not detected. Values represent average ± SD (*n* = 3 biological replicates).

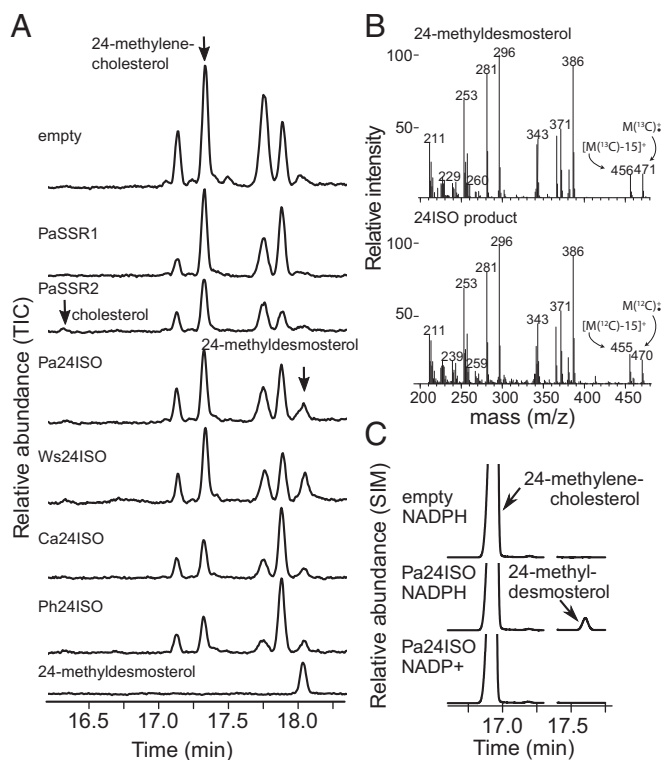


Fig. 5. The 24ISO catalyzed conversion of 24-methylenecholesterol to 24-methylidesmosterol in yeast. (A) Sterol extracts from *S. cerevisiae* strain T21 expressing DWF1 homologs analyzed by GC-MS (TIC, total ion chromatogram); 24-methylidesmosterol standard is shown at the bottom. Selected ion monitoring (SIM) is shown in *SI Appendix, Fig. S3*. (B) MS spectra of trimethylsilylated [26- ^{13}C]-labeled 24-methylidesmosterol standard (Top) and 24ISO product (Bottom). The molecular ion of trimethylsilylated ^{13}C -24-methylidesmosterol is m/z 471 ($399 + 72$), while the m/z 456 mass corresponds to the demethylated ion from the molecular ion. The corresponding ions of the in vivo-synthesized 24-methylidesmosterol are m/z 470 ($398 + 72$) and m/z 455. (C) In vitro assay using Pa24ISO expressed in *S. cerevisiae* strain *erg4* and 24-methylenecholesterol as substrate. SIM for 24-methylenecholesterol: m/z 296, 365, 386 and 24-methylidesmosterol: m/z 296, 343, 386.

involved in C-24 alkylsterol biosynthesis. Solanaceous plants appear to have acquired *SSR2* by gene duplication from *DWF1/SSR1* (Fig. 7), which enables increased production of cholesterol relative to other plants (11). Although the role of cholesterol in the Solanaceae is unknown, *Solanum* plants, such as potato and tomato, use cholesterol as a substrate in the biosynthesis of steroidal glycoalkaloids (11). Another duplication seems to have occurred from *SSR2*, giving rise to *24ISO* (Fig. 7), which in withanolide-producing plants is involved in the biosynthesis of these compounds. *SSR1* catalyzes a two-step reaction: $\Delta^{24(28)}$ to $\Delta^{24(25)}$ -isomerization followed by reduction of the double bond. It would therefore be easy to assume that *24ISO* is a paralog of *SSR1* that has lost the second-step reduction reaction. Interestingly, our phylogenetic analysis revealed that *24ISO* is derived from *SSR2* [$\Delta^{24(25)}$ -reductase], not *SSR1*. Moreover, *24ISO* also has weak $\Delta^{24(25)}$ -reduction activity. Based on our data we suggest that *24ISO* has reacquired the $\Delta^{24(28)}$ to $\Delta^{24(25)}$ -isomerization activity after diverging from *SSR2*. Alternatively, the genetic precursor to *SSR2* may have been less specific than the modern version, and the separation of reductase and isomerase activities in *SSR2* and *24ISO* was acquired independently after the duplication event.

Surprisingly, this isomerization reaction requires NADPH that cannot be replaced by NADP⁺, even though no net reduction takes place. A requirement for NADPH by an isomerase has also been

described for the unrelated enzyme isopentenyl diphosphate isomerase 2, where reduced FMN acts as both acid and base to facilitate proton transfers (36, 37). As another example, the isomerization reaction catalyzed by human type I β -hydroxysteroid dehydrogenase/isomerase requires NADH, which induces conformational changes in the enzyme structure as the isomerase activity reaches a maximum (38). However, *24ISO* does not share any common domains with human type I β -hydroxysteroid dehydrogenase/isomerase. Further analysis of the reaction mechanism of *24ISO* could reveal a novel mechanism of isomerase activity.

Since *24ISO/SSR-like* occurs in members of the Solanoideae subfamily as well as in *Petunia*, but not in any *Nicotiana* species sequenced so far, a parsimonious hypothesis could be that *24ISO/SSR-like* originated in a common ancestor of Nicotianoideae, Petunioideae, and Solanoideae, with a subsequent loss in, for example, Nicotianoideae and members of Solanum, although we need to entertain the possibility of other more complex evolutionary hypotheses. As we show similar activities for Ph24ISO and Ws24ISO (Fig. 5A and *SI Appendix, Fig. S3*), and in vitro synthesis of petuniasterones uses 24-methylidesmosterol as precursor (35), the suggested hypothesis only involves one neofunctionalization, namely the transfer from a $\Delta^{24(25)}$ reductase to a $\Delta^{24(28)}$ to $\Delta^{24(25)}$ isomerase (Fig. 7).

Solanum species accumulate steroidal glycoalkaloids, a different specialized metabolite of steroidal origin (39), and may have lost *24ISO/SSR-like* due to production of putative functionally redundant steroidal glycoalkaloids. Solanum species generally produce either one of the specialized metabolites, withanolides or steroidal glycoalkaloids, presumably due to evolutionary pressure to preserve energy resources. Cooccurrence of steroidal glycoalkaloids and withanolide-type compounds has only been described in two cases: *S. ciliatum* and *S. sisymbriifolium* (19, 20). The hypothesis that plants either produce 24-methylidesmosterol or cholesterol-derived specialized metabolites is further supported by our finding that *SSR2* is not expressed or has low expression levels in plants that express *24ISO*.

Interestingly, withanolides and, correspondingly, *24ISO* are absent in the crop plants in the Solanum genus. The *24ISO* is missing from the genomes of potato and tomato, only remains as a pseudogene in *S. melongena*, and is not expressed in *C. annuum* aerial tissues. We cannot draw any firm conclusions based on our limited dataset, but our data suggest that *24ISO* was selected against in the domestication of Solanum crop plants, leading to absence of withanolides in these species.

Withanolides give solanaceous plants alternative defense compounds against insects feeding on plants of this family. While steroidal glycoalkaloids are potent antifeedants (40), withanolides may provide protection from insect pests resistant to steroidal glycoalkaloids (41). This observation further supports the idea that withanolides differ in functionality from steroidal glycoalkaloids. The paralogous functions of *24ISO* and *SSR2* contribute to maximizing chemodiversity of solanaceous plants with minimal evolutionary change.

A few other plants outside of the Solanaceae have been reported to produce withanolides: *Cassia siamea* (42), *Ajuga parviflora* (43), *Ajuga bracteosa* (44), *Eucalyptus globulus* (45), and *Tacca plantaginea* (46, 47). Withanolides have also been identified in soft corals (48–50). We could only identify one DWF1 homolog in the available transcriptome for *Ajuga reptans* (1KP) (21) and genome for *Eucalyptus grandis* (51), suggesting that these other species might have acquired the ability to produce withanolides through convergent evolution, using a different pathway for withanolide biosynthesis.

We show here that *24ISO* is a key enzyme in the production of withanolides from 24-methylenecholesterol in the Solanoideae subfamily and petunia species. The Solanoideae subfamily contains several medicinal plants. Up-regulation of *24ISO* activity would channel more substrate into the withanolide biosynthetic pathway and be a useful tool for the sustainable production of pharmacologically active withanolides in plants. Based on the fact

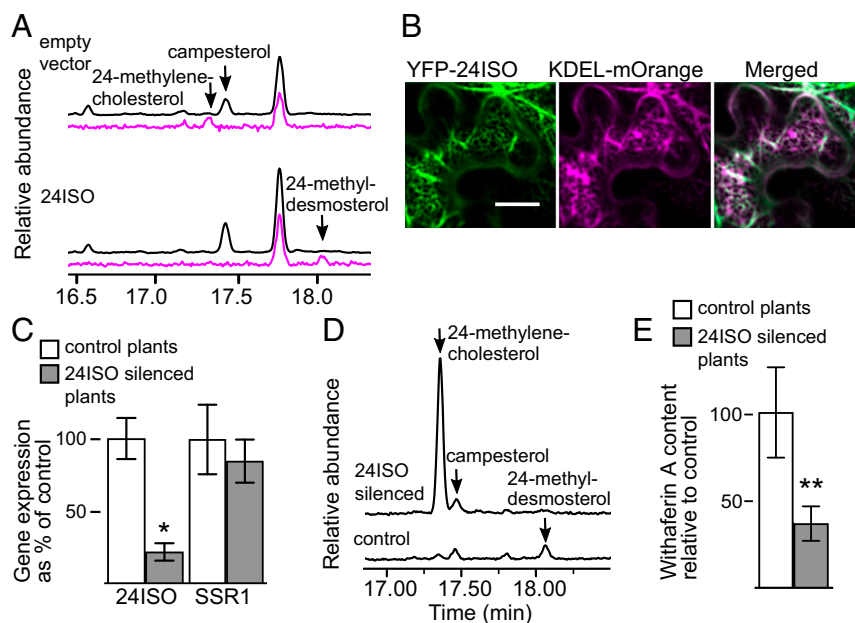


Fig. 6. *In planta* experiments showed 24ISO to be involved in withanolide biosynthesis. (A) Sterol profile in tobacco leaves expressing Pa24ISO analyzed by GC-MS. TIC is shown in black and extracted ion chromatogram for m/z 296 in magenta. (B) Subcellular localization of YFP-Pa24ISO (green) and ER-marker KDEL-mOrange (magenta). (Scale bar, 20 μ m.) Localization of Ws-, Ca-, and Ph24ISO are shown in *SI Appendix, Fig. S4*. (C) Expression levels of 24ISO and SSR1 in control (white bars) and 24ISO silenced (gray bars) *W. somnifera* plants. SSR2 expression levels were below detection limit in both control plants and 24ISO-silenced plants. Values represent average of six independent lines \pm SD. * $P = 6.5 \times 10^{-6}$ (Student's t test). Values for individual lines are shown in *SI Appendix, Fig. S6A*. (D) GC-MS analysis showing TIC of sterol extracts from *W. somnifera* leaves silenced in 24ISO (VIGS). Relative content of 24-methylenecholesterol and 24-methyl-desmosterol for individual lines and scatter plots showing 24ISO gene expression and metabolite accumulation are shown in *SI Appendix, Fig. S6 B and C*. (E) Withaferin A content in 24ISO-silenced plants relative to control plants analyzed by LC-QTOF-MS. Values represent average of six independent lines \pm SD. ** $P = 0.001$. Withaferin A content in individual lines and a scatter plot of 24ISO gene expression and withaferin A content are shown in *SI Appendix, Fig. S6 D and E*. TIC and MS/MS spectra of representative samples and withaferin A standard are shown in *SI Appendix, Fig. S7*.

that 24ISO evolved by duplication from an enzyme of the general phytosterol pathway, and that several enzymes involved in cholesterol biosynthesis are also derived from general phytosterol metabolism (13), we suggest that later enzymes in the withanolide biosynthetic pathway are also found among homologs of general phytosterol metabolism enzymes. As shown in Fig. 3, there are possible gene clusters surrounding 24ISO in the genomes of three Solanaceae plants. Thus, *W. somnifera* homologs to the cytochrome P450 and 2OGD genes found in these genomic regions are good candidates for downstream metabolic genes.

Material and Methods

Plant Materials. Seeds of *P. alkekengi* var. *Franchetii*, *S. melongena* var. *Senryo no. 2*, and *C. annuum* var. *Tachiyatsufusa* were purchased at local garden centers. Seeds of *W. somnifera* were purchased from Shanti Garden Nursery (shanti-g.com). Seeds of *P. hybrida* inbred line V26 from stock in our laboratory. Plants were grown in soil at 22 °C and 16 h light/8 h dark.

Phylogenetic Analysis. We performed BLAST analysis on our previously published *P. alkekengi* and *P. peruviana* transcriptome datasets (14), using StSSR1 and StSSR2 as queries. This yielded three sequences in each species, SSR1, SSR2, and 24ISO. Pa24ISO was used as a query in BLAST analyses against solanaceous plants at the NCBI (<https://blast.ncbi.nlm.nih.gov/Blast.cgi>), the Sol Genomics (<https://solgenomics.net/>), and 1KP (21) databases. The extracted sequences and their accession numbers are given in *SI Appendix, Table S1* and *Dataset S1*. For *W. somnifera*, we performed reanalysis of published leaf and root transcriptome datasets (accession numbers SRA053485 and SRP040231) (15, 16). Data preprocessing, filtering, de novo transcriptome assembly, and the functional annotation were carried out according published procedures (14, 52). The genomes of *C. annuum*, *S. melongena*, and *P. hybrida* were accessed at The Pepper Genome Database (24), The Eggplant Genome Project (25), and the Sol Genomics Network.

Protein sequences were aligned using CLUSTALW embedded in MEGA7 (53). A maximum likelihood tree was inferred in MEGA7 with bootstrap method (1,000 replicates). *Arabidopsis* DWF1 was used to root the tree.

Sterol Analysis. Phytosterol extraction was modified from Itkin et al. (54). Fifty milligrams of frozen, powdered plant material was extracted in 2 mL choloform/MeOH (2:1 vol/vol) at 75 °C for 1 h. After 1 h at room temperature, the solvent was evaporated in a vacuum concentrator. The dried residue was saponified in 500 μ L 6% (wt/vol) KOH in MeOH for 1 h at 90 °C. After samples cooled to room temperature, 500 μ L H₂O and 500 μ L *n*-hexane were added, shaken for 30 s, and centrifuged briefly to separate the phases. The hexane phase was transferred to a clean 1,500- μ L Eppendorf tube and dried in a vacuum concentrator. The remaining aqueous phase was extracted twice more with 500 μ L *n*-hexane, which was added to the dried first extract and dried. Dried samples were resuspended in 50 μ L *N*-methyl-*N*-trimethylsilyl trifluoroacetamide (Sigma), transferred to 2-mL glass vials with a 100- μ L glass insert containing 0.01 μ g 5- α -cholestane (Sigma), and incubated at room temperature at least 15 min before analysis.

GC-MS analysis was performed on a Shimadzu GCMS-TQ8040 with a DB-1 (30 m \times 0.25 mm, 0.25- μ m film thickness; Agilent) or HP-5 (30 m \times 0.32 mm,

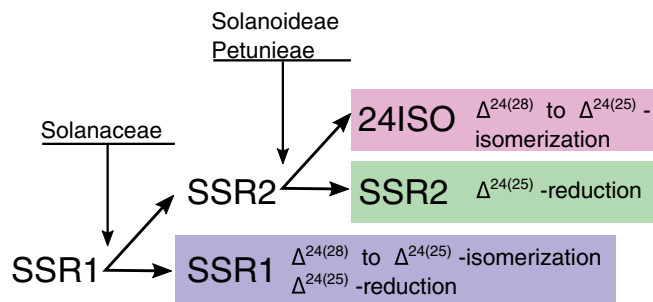


Fig. 7. The evolution of three DWF1 paralogs, SSR1, SSR2, and 24ISO/SSR-like, in the Solanaceae. SSR1 and SSR2 are found in all solanaceous plants originating from a duplication event in a common ancestor to this family. A later duplication event in a common ancestor of the Solanoideae gave rise to 24ISO/SSR-like from SSR2.

0.25- μm film thickness; SGE Analytical Science) capillary column following the method described by Seki et al. (27) with modifications. Injection temperature was set at 250 °C with a split ratio of 15. Temperature program was as follows: 80 °C for 1 min followed by temperature increase to 300 °C at a rate of 20 °C/min and hold at 300 °C for 10–28 min. Cholesterol, campesterol, stigmasterol, and β -sitosterol were identified based on authentic standards purchase from Tama Biochemical Co. Authentic standards for 24-methylenecholesterol and [26-¹³C]-labeled 24-methyl-desmosterol were prepared with their structural confirmation in the previous study (55, 56). Quantification of sterols was based on a standard calibration curve of authentic standards.

Quantitative Reverse-Transcription PCR. RNA was extracted using RNeasy Plant Mini Kit (Qiagen). cDNA was synthesized using the SuperScript III first-strand synthesis system (Invitrogen). Real-time PCR was done with the StepOnePlus Real-Time PCR system using Fast SYBR Green Master Mix (Applied Biosystems). Transcripts were quantified using plasmid DNA containing the corresponding gene. Primers used in the analysis are given in *SI Appendix, Table S2*. For the transcript profiling of *24ISO*, *SSR1*, and *SSR2* in various plants and tissues, three biological replicas were analyzed. For the analysis of *24ISO* expression in VIGS plants, six biological replicas were analyzed.

Cloning of Genes and Plasmid Construction. RNA was isolated from leaves of *P. alkekengi*, *P. hybrida*, *W. somnifera*, *C. annuum*, and *S. melongena* using the Plant RNeasy mini kit (Qiagen) and cDNA synthesized with the SuperScript First-Strand Synthesis System for RT-PCR (Life Technologies). Since PaSSR2 was not expressed, it was cloned from gDNA extracted from *P. alkekengi* leaves using DNeasy plant mini kit (Qiagen). The intron was removed by overlap PCR. PCR products were cloned into pENTR/D-TOPO (Invitrogen) and sequences verified. Primers used for cloning are given in *SI Appendix, Table S2*. Expression clones were generated by Gateway cloning into pYES-DEST52 for expression in *Saccharomyces cerevisiae* and pGWB8 (57) for transient expression in *N. benthamiana*.

Yeast in Vivo Assays. The 24-methylenecholesterol-producing *S. cerevisiae* strain T21 and desmosterol-producing *S. cerevisiae* strain T31 (11) were transformed with pYES-DEST52-PaSSR1, -PaSSR2, -Pa24ISO, -Ph24ISO, -Ws24ISO, -Ca24ISO, and -Sm24ISO. pYES-DEST52 without insert was used as empty vector control. Transformed yeast was cultured and analyzed as previously described (11). Five hundred microliters of ethyl acetate was added to harvested cells and they were disrupted by sonication. The extraction step was repeated twice. The ethyl acetate fraction was washed with 1 mL water, dried in vacuum, and analyzed by GC-MS after trimethylsilylation as described above.

In Vitro Activity Assays. *S. cerevisiae* BY4742 *erg4* (58) (Open Biosystems) was transformed with pYES-DEST52-PaSSR1, -PaSSR2, -Pa24ISO, -Ph24ISO, -Ws24ISO, -Ca24ISO, -Sm24ISO, or empty pYES-DEST52 and in vitro enzyme activity was assayed as previously described (11). In short, harvested cells were resuspended in 20 mM Tris-HCl, pH 7.5, and 50 mM NaCl and disrupted using 0.5-mm glass beads in a Beadbeater (BioSpec Products). Protein concentration in the cleared lysate was measured with Quick Start Bradford Protein Assay 2 (Bio-Rad) using BSA as standard. Enzyme activity in crude extracts was assayed in 0.5-mL reaction mixtures containing 0.3 mg·mL⁻¹ protein homogenate, 0.5 mg·mL⁻¹ BSA, 100 mM Tris-HCl, pH 7.23, 1 mM DTT, 20 μM flavin adenine nucleotide, 2 mM NADPH, and 168 μM sterol substrate (sources as given above). Samples were incubated overnight at 30 °C and extracted three times with 0.5 mL *n*-hexane. Extracts were dried, trimethylsilylated, and analyzed by GC-MS as described above.

To test NADPH/NADP⁺ requirement, His-fusion protein was semipurified using TALON metal affinity resin (Clontech) to remove background NADP reducing activity from the yeast crude extracts. The purified protein was used in in vitro assays as described above, with either 2 mM NADPH or 2 mM

NADP⁺ in the assay mix. To measure NADPH consumption, absorbance at 340 nm was measured before and after overnight incubation.

Heterologous Expression in *N. benthamiana*. Leaves of 4-wk-old *N. benthamiana* plants were transformed by agroinfiltration (59). *Agrobacterium tumefaciens* strain GV3101 (pMP90) carrying pGWB5-PaSSR1, -PaSSR2, -Pa24ISO, -Ph24ISO, -Ca24ISO, -Ws24ISO, or -Sm24ISO vector were coinfiltrated with *Agrobacterium* carrying the p19 silencing suppressor (each OD₆₀₀ = 0.5). *Agrobacterium* carrying p19 was infiltrated alone for the negative control. Six days after transformation, sterols were extracted and analyzed by GC-MS as described above.

Subcellular Localization of Transiently Expressed 24ISO in Leaves of *N. benthamiana*. Full-length 24ISO gene sequences were PCR-amplified and cloned into pJET 1.2/blunt cloning vector following the manufacturer's instructions and then by LR reaction moved to pEarleyGate 104 vector for transient plant expression of N-term YFP fused constructs (60). The ER marker KDEL-mOrange plant expression vector was kindly provided by Tonni Andersen, Université de Lausanne, Lausanne, Switzerland. Expression constructs were transformed into the *A. tumefaciens* strain pGV3850 and *Agrobacterium*-mediated transient transformation of *N. benthamiana* leaves was carried out as described above. The *Agrobacterium* strains harboring the appropriate construct (OD₆₀₀ = 0.2) were coinfiltrated with the strain harboring the p19 construct (OD₆₀₀ = 0.1). Image acquisition was performed with a Leica SP5 confocal laser scanning microscope (Leica Microsystems GmbH) equipped with a 63 \times objective lens using YFP and RFP filter setting provided by Leica.

VIGS. Gene silencing was done using a tobacco rattle virus (TRV)-based VIGS system (61). Inserts were cloned into pTRV2 using EcoRI and KpnI restriction sites and the resulting plasmids cloned into *Agrobacterium* strain GV2260 transformed with GabT, provided by Satoko Nonaka, University of Tsukuba, Tsukuba, Japan (62). Phytoene desaturase (PDS) was used to verify VIGS and to determine time of harvest. pTRV2 containing a fragment of GFP was used as negative control. Three short sequences from *Ws24ISO* were cloned individually and assembled into pTRV2 to yield the *24ISO* targeting construct (details given in *SI Appendix, Fig. S5* and *Table S2*). The leaves of 3-wk-old *W. somnifera* seedlings were infiltrated with *Agrobacterium* harboring pTRV1 and pTRV2 in a 1:1 ratio by syringe infiltration. Six individual plants were infiltrated per construct, and silencing of target gene was confirmed by qPCR at time of harvest in all infiltrated plants. Bleaching of PDS control plants was observed about 3 wk after infiltration and samples were harvested about 4 wk after infiltration. The five top leaves from each plant were harvested and pooled for one sample, and aliquots of the same sample were used for qPCR, GC-MS, and LC-MS analysis.

Withanolide Analysis. Withanolide extraction from control and *24ISO*-silenced plants and analysis of withanolides by LC-QTOF-MS were done as described previously (14). Withaferin A was identified based on MS/MS data compared with that of authentic standard withaferin A (Sigma). Six biological replicas were analyzed for both control and VIGS plants.

ACKNOWLEDGMENTS. We thank Yasuhiro Katoda and Ken Shirasu (RIKEN) for their help with VIGS and providing the pTRV2-GFP control vector, Tetsuya Sakurai and Yutaka Yamada (RIKEN) for computational assistance, Tonni Andersen (Université de Lausanne) for providing the KDEL-mOrange plant expression vector, and Satoko Nonaka and Hiroshi Ezura (Tsukuba University) for providing the gabT construct. E.K. was supported by the Carlsberg Foundation and the Japan Society for the Promotion of Science (JSPS). This research was supported, in part, by grants-in-aid, JSPS KAKENHI for JSPS Fellows.

- Thimmappa R, Geisler K, Louveau T, O'Maille P, Osbourn A (2014) Triterpene biosynthesis in plants. *Annu Rev Plant Biol* 65:225–257.
- Misico RI, et al. (2011) Withanolides and related steroids. *Progress in the Chemistry of Organic Natural Products* (Springer, Vienna), pp 127–216.
- Mishra L-C, Singh BB, Dagenais S (2000) Scientific basis for the therapeutic use of Withania somnifera (ashwagandha): A review. *Altern Med Rev* 5:334–346.
- White PT, Subramanian C, Motiwala HF, Cohen MS (2016) Natural withanolides in the treatment of chronic diseases. *Anti-Inflammatory Nutraceuticals and Chronic Diseases*, eds Gupta SC, Prasad S, Aggarwal BB (Springer, Cham, Switzerland), pp 329–373.
- Glotter E (1991) Withanolides and related ergostane-type steroids. *Nat Prod Rep* 8:415–440.
- Lockley WJS, Rees HH, Goodwin TW (1976) Biosynthesis of steroidal withanolides in *Withania somnifera*. *Phytochemistry* 15:937–939.
- Andrews-Smith W, Gill HK, Smith RW, Whiting DA (1991) Stages in the biosynthesis of the epoxy lactol side chain of Nic-1, insect antifeedant steroid of *Nicandra physaloides*. *J Chem Soc Perkin Trans 1*, 291–296.
- Klahre U, et al. (1998) The Arabidopsis DIMINUTO/DWARF1 gene encodes a protein involved in steroid synthesis. *Plant Cell* 10:1677–1690.
- Choe S, et al. (1999) The Arabidopsis dwarf1 mutant is defective in the conversion of 24-methylenecholesterol to campesterol in brassinosteroid biosynthesis. *Plant Physiol* 119:897–907.
- Takahashi K, et al. (2006) Metabolic conversion of 24-methyl- Δ 25-cholesterol to 24-methylcholesterol in higher plants. *Bioorg Med Chem* 14:732–738.
- Sawai S, et al. (2014) Sterol side chain reductase 2 is a key enzyme in the biosynthesis of cholesterol, the common precursor of toxic steroidal glycoalkaloids in potato. *Plant Cell* 26:3763–3774.
- Waterham HR, et al. (2001) Mutations in the 3 β -hydroxysterol Delta24-reductase gene cause desmosterolosis, an autosomal recessive disorder of cholesterol biosynthesis. *Am J Hum Genet* 69:685–694.
- Sonawane PD, et al. (2016) Plant cholesterol biosynthetic pathway overlaps with phytosterol metabolism. *Nat Plants* 3:16205.

14. Fukushima A, et al. (2016) Comparative characterization of the leaf tissue of *Physalis alkekengi* and *Physalis peruviana* using RNA-seq and metabolite profiling. *Front Plant Sci* 7:1883.
15. Gupta P, et al. (2013) De novo assembly, functional annotation and comparative analysis of *Withania somnifera* leaf and root transcriptomes to identify putative genes involved in the withanolides biosynthesis. *PLoS One* 8:e62714.
16. Senthil K, et al. (2015) Transcriptome analysis reveals in vitro cultured *Withania somnifera* leaf and root tissues as a promising source for targeted withanolide biosynthesis. *BMC Genomics* 16:14.
17. Eich E (2008) *Solanaceae and Convolvulaceae—Secondary Metabolites: Biosynthesis, Chemotaxonomy, Biological and Economic Significance: A Handbook* (Springer, Berlin).
18. Suleiman RK, Zarga MA, Sabri SS (2010) New withanolides from *Mandragora officinarum*: First report of withanolides from the genus *Mandragora*. *Fitoterapia* 81: 864–868.
19. Zhu XH, Takagi M, Ikeda T, Midzuki K, Nohara T (2001) Withanolide-type steroids from *Solanum cilistum*. *Phytochemistry* 56:741–745.
20. Niero R, et al. (2006) Cilistepoxide and cilistadiol, two new withanolides from *Solanum sisymbriifolium*. *Nat Prod Res* 20:1164–1168.
21. Matasci N, et al. (2014) Data access for the 1,000 Plants (1KP) project. *Gigascience* 3:17.
22. Elliger CA, et al. (1988) Petunasterones, novel ergostane-type steroids of *Petunia hybrida* Vilm. (Solanaceae) having insect-inhibitory activity. X-ray molecular structure of the 22,24,25-[(methoxycarbonyl)orthoacetate] of 7 α ,22,24,25-tetrahydroxy ergosta-1,4-dien-3-one and of 1 α -acetoxy-24,25-epoxy-7 α -hydroxy-22-(methylthiocarbonyl)acetoxycergosta-3-one. *J Chem Soc Perkin Trans 1*, 711–717.
23. Rozkrutowa B (1987) Phytochemical investigation on *Browallia viscosa*. *Proceedings of the 3rd Conference on Chemistry and Biotechnology of Biologically Active Natural Products* (Wiley-VCH, Weinheim, Germany), pp 178–181.
24. Qin C, et al. (2014) Whole-genome sequencing of cultivated and wild peppers provides insights into Capsicum domestication and specialization. *Proc Natl Acad Sci USA* 111:5135–5140.
25. Giuliano G (2017) The eggplant genome reveals key events in Solanaceae evolution. Available at <https://pag.confex.com/pag/xxv/meetingapp.cgi/Paper/23484>. Accessed July 26, 2018.
26. Helliwell CA, Chandler PM, Poole A, Dennis ES, Peacock WJ (2001) The CYP88A cytochrome P450, ent-kaurenic acid oxidase, catalyzes three steps of the gibberellin biosynthesis pathway. *Proc Natl Acad Sci USA* 98:2065–2070.
27. Seki H, et al. (2008) Licorice beta-amyrin 11-oxidase, a cytochrome P450 with a key role in the biosynthesis of the triterpene sweetener glycyrrhizin. *Proc Natl Acad Sci USA* 105:14204–14209.
28. Itkin M, et al. (2013) Biosynthesis of antinutritional alkaloids in solanaceous crops is mediated by clustered genes. *Science* 341:175–179.
29. Nakayasu M, et al. (2017) A dioxygenase catalyzes steroid 16 α -hydroxylation in steroidal glycoalkaloid biosynthesis. *Plant Physiol* 175:120–133.
30. Bombarely A, et al. (2016) Insight into the evolution of the Solanaceae from the parental genomes of *Petunia hybrida*. *Nat Plants* 2:16074.
31. Silvestro D, Andersen TG, Schaller H, Jensen PE (2013) Plant sterol metabolism. $\Delta(7)$ -Sterol-C5-desaturase (STE1/DWARF7), $\Delta(5,7)$ -sterol- $\Delta(7)$ -reductase (DWARF5) and $\Delta(24)$ -sterol- $\Delta(24)$ -reductase (DIMINUTO/DWARF1) show multiple subcellular localizations in *Arabidopsis thaliana* (Heynh) L. *PLoS One* 8:e56429.
32. Lavie D, Glotter E, Shvo Y (1965) Constituents of *Withania somnifera* Dun. III. The side chain of Withaferin A. *J Org Chem* 30:1774–1778.
33. Scossa F, Benina M, Alseekh S, Zhang Y, Fernie AR (May 29, 2018) The integration of metabolomics and next-generation sequencing data to elucidate the pathways of natural product metabolism in medicinal plants. *Planta Med*, 10.1055/a-0630-1899.
34. Saema S, ur Rahman L, Niranjana A, Ahmad IZ, Misra P (2015) RNAi-mediated gene silencing of WsSGTL1 in *W. somnifera* affects growth and glycosylation pattern. *Plant Signal Behav* 10:e1078064.
35. Faraldos JA, Giner JL (2002) Biomimetic synthesis of petuniasterone D via the epoxy ester-ortho ester rearrangement. *J Org Chem* 67:4659–4666.
36. Calveras J, Thibodeaux CJ, Mansoorabadi SO, Liu HW (2012) Stereochemical studies of the type II isopentenyl diphosphate-dimethylallyl diphosphate isomerase implicate the FMN coenzyme in substrate protonation. *ChemBioChem* 13:42–46.
37. Thibodeaux CJ, Mansoorabadi SO, Kittleman W, Chang WC, Liu HW (2008) Evidence for the involvement of acid/base chemistry in the reaction catalyzed by the type II isopentenyl diphosphate/dimethylallyl diphosphate isomerase from *Staphylococcus aureus*. *Biochemistry* 47:2547–2558.
38. Thomas JL, et al. (2003) Structure/function relationships responsible for coenzyme specificity and the isomerase activity of human type 1 3 β -hydroxysteroid dehydrogenase/isomerase. *J Biol Chem* 278:35483–35490.
39. Heftmann E (1983) Biogenesis of steroids in Solanaceae. *Phytochemistry* 22: 1843–1860.
40. Milner SE, et al. (2011) Bioactivities of glycoalkaloids and their aglycones from *Solanum* species. *J Agric Food Chem* 59:3454–3484.
41. Elliger CA, Waiss AC (1989) Insect growth inhibitors from *Petunia* and other Solanaceous plants. *Pesticides of Plant Origin*, ACS Symposium Series, eds Arnason JT, Philogène BJR, Morand P (American Chemical Society, Washington, DC), Vol 387, pp 188–205.
42. Srivastava C, Siddiqui IR, Singh J, Tiwari HP (1992) An antifeedant and insecticidal steroid and a new hydroxyketone from *Cassia siamea* bark. *J Indian Chem Soc* 69:111.
43. Khan PM, Malik A, Ahmad S, Nawaz HR (1999) Withanolides from *Ajuga parviflora*. *J Nat Prod* 62:1290–1292.
44. Riaz N, Malik A, Nawaz SA, Muhammad P, Choudhary MI; Aziz-ur-Rehman (2004) Cholinesterase-inhibiting withanolides from *Ajuga bracteosa*. *Chem Biodivers* 1: 1289–1295.
45. Vankar PS, Srivastava J, Molčanov K, Kojic-Prodić B (2009) Withanolide A series steroidal lactones from *Eucalyptus globulus* bark. *Phytochem Lett* 2:67–71.
46. Liu H-Y, et al. (2006) Five new withanolides from *Tacca plantaginea*. *Chem Pharm Bull* 54:992–995.
47. Yang JY, Chen CX, Zhao RH, Hao XJ, Liu HY (2011) Plantagiolide F, a minor withanolide from *Tacca plantaginea*. *Nat Prod Res* 25:40–44.
48. Chao CH, et al. (2011) Paraminabeolides A-F, cytotoxic and anti-inflammatory marine withanolides from the soft coral *Paraminabea acronocephala*. *J Nat Prod* 74: 1132–1141.
49. Huang CY, et al. (2017) Bioactive new withanolides from the cultured soft coral *Sinularia brassica*. *Bioorg Med Chem Lett* 27:3267–3271.
50. Ksebati MB, Schmitz FJ (1988) Minabeolides: A group of withanolides from a soft coral, *Minabea* sp. *J Org Chem* 53:3926–3929.
51. Myburg AA, et al. (2014) The genome of *Eucalyptus grandis*. *Nature* 510:356–362.
52. Fukushima A, Nakamura M, Suzuki H, Saito K, Yamazaki M (2015) High-throughput sequencing and de novo assembly of red and green forms of the *Perilla frutescens* var. *crispa* transcriptome. *PLoS One* 10:e0129154.
53. Kumar S, Stecher G, Tamura K (2016) MEGA7: Molecular evolutionary genetics analysis version 7.0 for bigger datasets. *Mol Biol Evol* 33:1870–1874.
54. Itkin M, et al. (2011) GLYCOALKALOID METABOLISM1 is required for steroidal alkaloid glycosylation and prevention of phytotoxicity in tomato. *Plant Cell* 23:4507–4525.
55. Maruyama S, Fujimoto Y, Morisaki M, Ikekawa N (1982) Mechanism of campesterol demethylation in insect. *Tetrahedron Lett* 23:1701–1704.
56. Fujimoto Y, et al. (1997) Stereochemistry of the reduction of 24-methyldestosterol to campesterol and dihydrobrassicasterol in higher plants. *Chem Commun*, 681–682.
57. Nakagawa T, et al. (2007) Development of series of gateway binary vectors, pGWBs, for realizing efficient construction of fusion genes for plant transformation. *J Biosci Bioeng* 104:34–41.
58. Kelly DE, Lamb DC, Kelly SL (2001) Genome-wide generation of yeast gene deletion strains. *Comp Funct Genomics* 2:236–242.
59. Leuzinger K, et al. (2013) Efficient agroinfiltration of plants for high-level transient expression of recombinant proteins. *J Vis Exp*, 50521.
60. Earley KW, et al. (2006) Gateway-compatible vectors for plant functional genomics and proteomics. *Plant J* 45:616–629.
61. Dinesh-Kumar SP, Anandalakshmi R, Marathe R, Schiff M, Liu Y (2003) Virus-induced gene silencing. *Plant Functional Genomics*, ed Grotewold E (Humana, Totowa, NJ), pp 287–293.
62. Nonaka S, et al. (2017) An *Agrobacterium tumefaciens* strain with gamma-aminobutyric acid transaminase activity shows an enhanced genetic transformation ability in plants. *Sci Rep* 7:42649.
63. Olmstead RG, et al. (2008) A molecular phylogeny of the Solanaceae. *Taxon* 57: 1159–1181.